

# Adsorption of Ionophores and of Their Cation Complexes at the Water/Chloroform Interface: A Molecular Dynamics Study of a [2.2.2]Cryptand and of Phosphoryl-Containing Podands

A. Varnek, L. Troxler and G. Wipff\*

**Abstract.** We report molecular dynamics simulations on ionophores of different topologies and on their complexes with alkali and alkaline-earth cations, with or without counterion, at the water/chloroform interface. As ionophores we consider two phosphoryl-containing podands (the “chainlike” monopodand MP and the “octopuslike” tripodand TP) and the bicyclic cryptand **222**. We find that all the solutes behave as surfactants: they remain adsorbed at the interface, without migrating to bulk phases. Their precise location and solvation depend on the nature and conformation of the ionophore, of the cation and of the counterion. Schemati-

cally, two types of solutes can be distinguished, depending on their hydrophilic/hydrophobic character. The first type (cryptand **222** and its complexes, or the [MP·K<sup>+</sup>] complex), which have a hydrophobic exterior, stay on the chloroform side of the interface and are partially hydrated by “water fingers”. The second type (free MP and TP, [MP·K<sup>+</sup>]Pic<sup>-</sup> and

[MP·Sr<sup>2+</sup>](Pic<sup>-</sup>)<sub>2</sub> complexes), which are more hydrophilic, are partitioned to a greater extent between the two liquid phases. The status of the ion pairs at the interface depends on the interplay between cation···anion and anion···solvent interactions. When cation–anion interactions are strong enough (as in [MP·Sr<sup>2+</sup>](Pic<sup>-</sup>)<sub>2</sub>), the ion pairs remain intimate. Otherwise they dissociate, leading to solvent-separated ion pairs adsorbed at the interface (in the [222·K<sup>+</sup>]Pic<sup>-</sup> complex) or to the migration of the anion to the water phase (in the [222·K<sup>+</sup>]Cl<sup>-</sup> complex).

## Keywords

extraction · interfaces · ionophores · molecular dynamics · counterion effect · solvation

## Introduction

Interfacial phenomena play a fundamental role in the transfer of metal cations from water to an organic solvent, mediated by ionophores. The precise nature of the interface is ill-defined and is expected to depend on the way the experiment is carried out. In the case of static interfaces, indirect information comes from interfacial tension measurements of water/organic solvent systems in presence of typical extractants.<sup>[1–3]</sup> For instance, for biphasic systems with organophosphorus molecules,<sup>[4]</sup> carbonic acids and ethers,<sup>[5]</sup> and macrocyclic compounds,<sup>[6]</sup> it is found that the interfacial tension decreases as the concentration of these solutes increases, as typically observed with surfactants. This suggests that these ionophores tend, like surfactants, to be adsorbed at the liquid/liquid interface. Their concentration at the interface should therefore be larger than in the adjacent bulk solvents. Another source of indirect information comes from the analysis of extraction kinetics, where the interfacial adsorption/desorption of extractants and their complexes at the liquid/liq-

uid interface is explicitly included in the mechanistic models.<sup>[2, 7, 8]</sup> Here, the systems are not static but generally agitated. At the microscopic level, adsorption of extractants at the interface supposedly facilitates the cation capture from the water phase, because its hydrophilic cation binding sites are likely to point towards the water phase, that is, towards the approaching cation. From a phenomenological point of view, the Gibbs's adsorption theorem and related Langmuir isotherms,<sup>[5]</sup> widely used in solvent extraction,<sup>[9]</sup> phase-transfer catalysis<sup>[10]</sup> and electrochemistry,<sup>[11]</sup> characterise the thermodynamics of adsorption, though without providing a clear picture of the interface. Physical surface-sensitive optical methods such as “second harmonic generation”,<sup>[13]</sup> resonance laser Raman spectroscopy and attenuated total reflectance spectroscopy<sup>[14]</sup> provide more insights into structural aspects, but data are still rather limited, especially in relation to the question of ion extraction.

Generally speaking, it is considered that the extent of adsorption, as measured by the excess of interfacial concentration of the solute over its concentration in the organic phase, depends on the nature of the ionophore, on its concentration in the bulk phase and on the nature of the organic phase. However, a consistent series of related experimental data are still lacking. As far as the ionophore is concerned, its conformation-dependent hydrophilic/hydrophobic character, related to its size, topology,

[\*] G. Wipff, A. Varnek, L. Troxler  
Laboratoire MSM, URA 422 CNRS, Institut de Chimie,  
4, rue B. Pascal, 67000 Strasbourg (France)  
Fax: Int. code + (388)41-6104

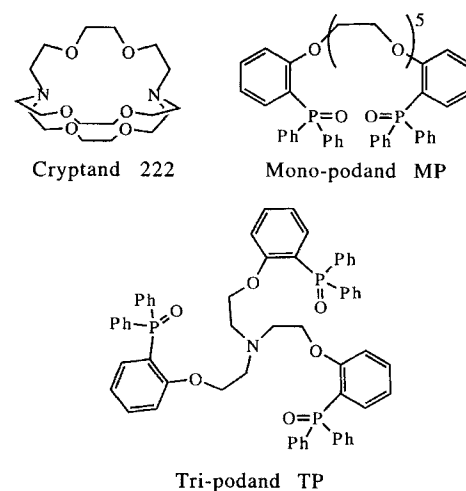
molecular constituents, orientation of binding sites and flexibility, should markedly determine the interfacial behaviour and mechanisms of carrier-mediated ion-crossing through the interface. However, based on existing experimental results, there is no clear description of adsorbed ionophores, and consistent investigations are still lacking.

Over the last decade these experimental limitations have stimulated the development of computational methods for modelling liquid/liquid interfaces with explicit representation of the solvents. Molecular dynamics (MD) or Monte Carlo simulations were first mostly performed on “neat” interfaces between water and benzene,<sup>[15]</sup> hexanol,<sup>[16]</sup> hexane,<sup>[17]</sup> nonane,<sup>[18]</sup> decane,<sup>[19]</sup> lipids<sup>[20]</sup> or extended hydrophobic interfaces.<sup>[21]</sup> These simulations showed that the interface is sharp at the molecular level, but not planar, and about 5 to 10 Å thick, with water hydrogen-bonding patterns that are somewhat different from those in bulk water. An important step was the simulation by Kessler et al. of molecular solutes such as squalene or fatty acids at a water/CCl<sub>4</sub> interface.<sup>[22]</sup>

Concerning the interface-crossing by ions, the first MD simulations looked into the migration of monoatomic ions (Cl<sup>-</sup>, F<sup>-</sup>, K<sup>+</sup> and Na<sup>+</sup>) from water to dichloroethane.<sup>[23]</sup> An interesting finding of Benjamin was that, despite the high affinity of these ions for water, there is a local energy minimum situated near the interface in the organic solvent.<sup>[23]</sup>

Recently we reported MD simulations on uncomplexed macrocyclic ionophores (the calix[4]arene anion, calix[4]arene-tetraamide, calix[4]-crown and -biscrown derivatives, and cryptand **222**)<sup>[24–28]</sup> at the chloroform/water interface. For timescales ranging from 300 to 600 ps, it was found that the ionophores that are initially equally shared by the two solvents are rapidly expelled out of the water phase, but remain in contact with the interface, without diffusing further into chloroform. The ionophores sitting almost entirely in chloroform bind to a few water molecules, which build up “water fingers”.<sup>[23, 29]</sup> Similar computational results were obtained for the M<sup>+</sup> alkali cation complexes of crown and biscrown derivatives of calix[4]arene and of alkali picrates M<sup>+</sup>Pic<sup>-</sup> complexes.<sup>[24–27]</sup> Acyclic ligands like CMPO's and their UO<sub>2</sub>(NO<sub>3</sub>)<sub>2</sub> complexes have also been recently simulated.<sup>[30]</sup>

In this paper, we compare the interfacial behaviour of three ionophores (**L**) possessing different molecular topologies: a “chainlike” monopodand **MP**, an “octopus-like” tripodand **TP** and the bicyclic cryptand **222**. Cryptand **222** selectively binds the K<sup>+</sup> cation in polar protic solvents or in extraction systems.<sup>[31]</sup> Numerous modelling studies have been devoted to its conformational and binding properties in water and non-aqueous solutions.<sup>[32–33]</sup> Podands **MP** and **TP** are newly synthesised molecules that combine polyether and phosphine oxide fragments.<sup>[35]</sup> Since mono- and bidentate phosphoryl-containing ligands (TOPO, TPPO, CMPO, etc.)<sup>[36]</sup> are widely used in industry to extract hard metal cations, remarkable extraction properties may be expected from the phosphoryl-containing podands **MP** and **TP**. Indeed, preliminary studies show that **MP** is a good extractant for the K<sup>+</sup>, Sr<sup>2+</sup> and Ba<sup>2+</sup> cations,<sup>[37]</sup> whereas **TP** efficiently complexes the Li<sup>+</sup> cation in acetonitrile.<sup>[35]</sup> Although the **222**, **MP** and **TP** ionophores are nearly insoluble in water,<sup>[31, 35, 37]</sup> their ether or phosphoryl binding sites may efficiently interact with this solvent at the water/



organic interface. However, since their hydrophobic/hydrophilic character depends markedly on their conformation,<sup>[32, 35, 38]</sup> it is not easy to predict how these molecules and their complexes behave at the interface.

More specifically, we report MD simulations at the water/chloroform interface on the free ionophores and on their complexes with alkali (Li<sup>+</sup>, K<sup>+</sup>) and alkaline-earth (Sr<sup>2+</sup>) metal cations, and with ion pairs M<sup>+</sup>X<sup>-</sup> and M<sup>2+</sup>(X<sup>-</sup>)<sub>2</sub> (X<sup>-</sup> = Pic<sup>-</sup>, Cl<sup>-</sup>), to gain insight into the microscopic picture of the interfacial behaviour of neutral and charged solutes, in the context of solvent extraction processes. A new important feature, compared to the our previous simulations, concerns the role of counterions on the interfacial behaviour. In order to save computer time, we selected typical complexes, instead of performing exhaustive comparisons.

## Method

We used the AMBER 4.1 software<sup>[39]</sup> for molecular mechanics and molecular dynamics simulations, with most of the parameters taken from ref. [40]. The atomic charges were derived for electrostatic potentials (ESP charges) on fragments of the **TP** and **MP** molecules (N-(C<sub>2</sub>H<sub>4</sub>OCH<sub>3</sub>)<sub>3</sub>, CH<sub>3</sub>O-C<sub>2</sub>H<sub>4</sub>-OCH<sub>3</sub> and CH<sub>3</sub>O-(C<sub>6</sub>H<sub>4</sub>)P(O)Ph<sub>2</sub>), calculated with the SPARTAN software<sup>[41]</sup> using a 6-31G\* basis set. They are given in Figure 1 and used for the free and complexed states of the ligands. For the cryptand **222**, the atomic charges were the same as in ref. [32], with no special scaling factor for 1...4 interactions. The same charges were used for the free and complexed ligands. The K<sup>+</sup> and Sr<sup>2+</sup> parameters are those derived by Åqvist from free energies

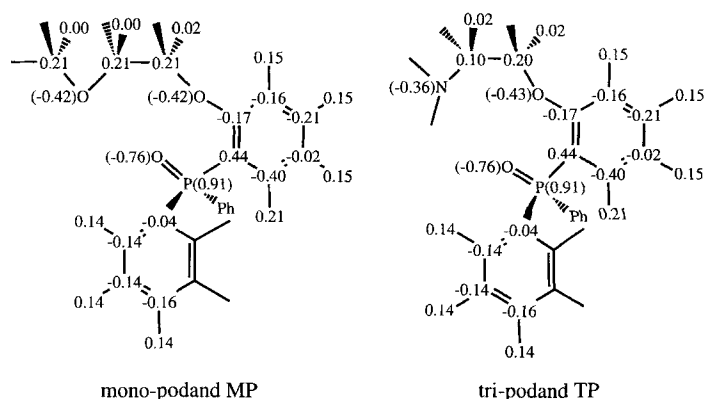


Figure 1. Atomic charges on **MP** and **TP**.

of hydration.<sup>[34]</sup> The solvent water and chloroform molecules were represented explicitly with the TIP3P<sup>[42]</sup> and the OPLS models,<sup>[43]</sup> respectively. In the case of chloroform the CH group is depicted in the united atom approximation.

Each phase was first equilibrated as a pure liquid. The solvent biphasic system was built from two adjacent "rectangular" boxes containing pure water and pure chloroform, respectively (Figure 2). The periodic boundary conditions were applied along all three directions as done by others.<sup>[15, 22]</sup> All solutes were first energy minimised in vacuo and immersed with their centre of mass at the centre of interface (Figure 2), while removing all solvent molecules with any atom closer than 3 Å and beyond 12, 12, 12 and 15 Å from the solute along the  $x$ ,  $y$ ,  $z_{\text{wat}}$  and  $z_{\text{chl}}$  axes, respectively (Figure 2). A density rescaling procedure was used before minimisation, in order to start with the experimental density of chloroform.

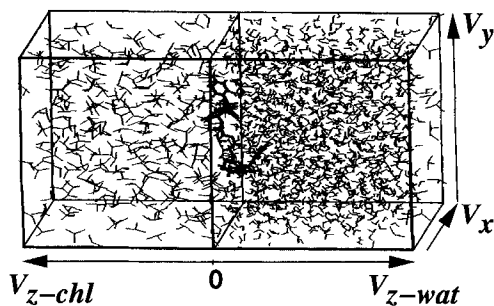


Figure 2. Schematic representation of the simulation box (chl = chloroform; wat = water).

After 1000 steps of conjugate gradient energy minimisation, the MD simulations were run for 200–850 ps at 300 K, using a time step of 1 fs. All bonds involving hydrogens and those of the solvent molecules were constrained with SHAKE. We performed the simulations in the NVT ensemble (i.e. constant number of particles  $N$ , temperature  $T$ , and volume  $V$ ). We used the Verlet algorithm, starting with random velocities at 300 K. The nonbonded interac-

tions were calculated with a residue based cut-off of 12 Å. The temperature was controlled by coupling to a thermal bath. The length of simulations, number of solvent molecules and sizes of the cell are presented in Table 1.

**Analysis of results:** The trajectories, saved every 0.2 ps, were analysed with the MDS and MD-DRAW software.<sup>[44]</sup> The position of the interface was defined as a coordinate  $z$  of intersection of the density curves of the two liquids, recalculated every 2 ps. The position of the solute with respect to the interface was defined by the  $z$  distance between its centre of mass and the  $z$  position of the interface (Table 1).

The solute–water and solute–chloroform interaction energies were recalculated from the MD trajectories. Their fluctuations are typically 10–12 kcal mol<sup>-1</sup>. The hydration of selected atoms  $A$  of the solute were characterised by the radial distribution functions (rdf)  $A \cdots O_{\text{water}}$  or  $A \cdots H_{\text{water}}$ . The coordination number of  $A$  was obtained by integration of the first peak of the rdf.

## Results

In all simulations we find that the solute remains adsorbed at the interface without migrating markedly into the bulk phase, but the precise adsorption patterns depend on the hydrophilic/hydrophobic character of the solute. Schematically, two types of solutes can be distinguished. The first type, represented by cryptand **222** and its cryptates or the  $[\text{TP} \cdot \text{Li}^+]$  complex, displays a hydrophobic exterior and migrates into chloroform, at 2–6 Å from the interface. It coordinates a few H<sub>2</sub>O molecules linked by a network of hydrogen bonds to the interfacial water ("water finger"<sup>[23, 29]</sup>). The second type of solute, represented by the free podands **MP** and **TP**, and by their complexes  $[\text{MP} \cdot \text{K}^+]\text{Pic}^-$  and  $[\text{MP} \cdot \text{Sr}^{2+}](\text{Pic}^-)_2$ , is more partitioned between the two phases, that is, some of the fragments are immersed in water and others in chloroform.

The solvation patterns and structure of the adsorbed species depend on the nature of the ionophore, of the cation and of the counterion. In this section we describe the behaviour of the free ionophores  $L$ , of their positively charged complexes  $[\text{L} \cdot \text{M}^+]$  and of complexes neutralised by counterions,  $[\text{L} \cdot \text{M}^+]\text{X}^-$  and  $[\text{L} \cdot \text{M}^{2+}](\text{X}^-)_2$ . Some of the conformers are characterised qualitatively by their "hydrophilic/hydrophobic" character, for simplicity. In the discussion section, we show how these computational results are consistent with related experimental data and discuss general features of the interfacial behaviour in relation to the hydrophobicity of the solute, and the important role of counterions.

**Adsorption of free ionophores at the interface:** *The cryptand 222:* This molecule has already been described in reference [28], but is reported briefly here for completeness. Two typical conformers of the free ionophore were considered: a hydrophilic one ( $K$  form) and a more hydrophobic one ( $II$  form), extracted, respectively, from the solid-state structures of the  $[\text{222} \cdot \text{K}^+]$  complex and of uncomplexed **222**. The  $II$  form, intrinsically the most stable, has no cavity, whereas the  $K$  form is preorganised for complexation. It was predicted that  $II$  would be more populous in apolar solvents and  $K$  in water.<sup>[32]</sup> At the water/chloroform interface, we found (see ref. [28] for details) that both forms move to the chloroform side of the interface. However, the  $II$  form, completely surrounded by chloroform molecules, has no contact with the water phase, and cannot therefore capture the  $\text{K}^+$  ion from water. This contrasts with the preorganised  $K$

Table 1. Free ionophores and ionophores complexed at the water/chloroform interface. Number of water ( $N_{\text{wat}}$ ) and chloroform ( $N_{\text{chl}}$ ) molecules in the simulated cell, dimensions of the cell ( $V_x$ ,  $V_y$ ,  $V_z$ ,  $V_{z-\text{wat}}$ ,  $V_{z-\text{chl}}$ , Å; see Figure 2), time simulated ( $t$ , ps) and average distance between the centre of mass of the solute and the interface ( $d$ , Å).

	$N_{\text{wat}}$	$N_{\text{chl}}$	$V_x$	$V_y$	$V_{z-\text{wat}}$	$V_{z-\text{chl}}$	$t$	$d$ [Å]
Free ionophores								
<b>222</b> $K$	538	140	25	24	27	34	600	-3.9 (4.1)
<b>222</b> $II$	503	125	26	22	27	32	400	-3.4 (3.8)
<b>TP</b> [b]	1675	374	45	41	28	30	250	+3.4 (1.1)
<b>TP</b> [c]	1397	277	38	38	30	20	50	+3.3 (1.0) [d]
<b>MP</b>	1323	286	40	37	28	28	300	+2.8 (1.0)
Charged complexes								
$[\text{222} \cdot \text{K}^+]\text{Pic}^-$	852	189	29	28	32	38	450	-1.9 (2.6)
$[\text{TP} \cdot \text{Li}^+]$	1397	277	38	38	30	20	200	-4.5 (1.2)
$[\text{MP} \cdot \text{K}^+]$	1396	245	37	35	28	28	150	+2.0 (0.9)
Neutral complexes								
$[\text{222} \cdot \text{K}^+]\text{Pic}^-$	1499	333	38	37	33	38	325	-4.6 (4.8)
$[\text{222} \cdot \text{K}^+]\text{Pic}^-$ [e]	808	252	23	33	24	45	850	-4.3 (2.7) [f]
$[\text{222} \cdot \text{K}^+]\text{Cl}^-$	736	185	29	28	28	34	60	-2.0 (0.9) [g]
$[\text{MP} \cdot \text{K}^+]\text{Pic}^-$	1321	266	38	36	30	28	300	+0.7 (0.4) [h]
$[\text{MP} \cdot \text{Sr}^{2+}](\text{Pic}^-)_2$	1328	272	39	37	30	28	350	+1.4 (0.9) [h]

[a] The signs + and - indicate that the centre of mass of the solute lies in water and chloroform, respectively. Standard deviations are given in parentheses. Unless specified,  $d$  was calculated over the whole dynamic run after skipping the first 50 ps. [b] "Open" starting structure ("hydrophilic" conformation 1; see text). [c] "Closed" starting structure ("hydrophobic" conformation 2; see text). [d] Averaged over last 10 ps of MD. [e] Starting with the complex immersed in bulk chloroform. [f] Because the solute  $[\text{222} \cdot \text{K}^+]$  diffuses from the bulk chloroform toward the interface, the average position  $d$  is reported over the last 50 ps. [g] Because of migration of the  $\text{Cl}^-$  anion to the bulk water, this distance is reported for  $[\text{222} \cdot \text{K}^+]$  only. [h] Averages are reported over the last 150 ps of MD.

form, which is directly coordinated with water molecules and is properly oriented to capture a cation.

**The phosphoryl-containing tripodand (TP):** Two simulations were performed, starting with different structures, which differed in their hydrophilic/hydrophobic character. The “hydrophilic” conformation 1 was taken from the last MD structure of the free ionophore in the gas phase. All its oxygens diverge from the pseudo- $C_3$  symmetry axis, and its phosphoryl groups, which have no preferential orientation, can be solvated by water (Figure 3a). In the “hydrophobic” conformation 2, extracted from the  $[TP \cdot Li^+]$  complex,<sup>[35]</sup> the three P=O groups converge towards the  $C_3$  symmetry axis, that is, towards the centre of the hydrophilic pseudocavity, while the aryl groups diverge. We found that the simulations at the interface starting with both conformers resulted in a similar final structure, close to conformation 1. There is no pseudocavity and all oxygens “diverge”, that is, point towards the solvent. The TP molecule is partitioned between the two phases. All three P=O groups are immersed in water, and each is hydrogen bonded to two water molecules (Figure 3b). This contrasts with the ether oxygens, which display no hydrogen bonding to interfacial water molecules.

**The phosphoryl-containing monopodand (MP):** Initially, the solute had a “flat” pseudocyclic conformation with antiparallel orientations of the two P=O groups. During the simulation, MP lost its cyclic shape (Figure 3c) and adopted a “snakelike” shape. The two phosphoryl groups are immersed in water and coordinated to 2–3 water molecules, while the ether oxygens are hydrated by 0.5–1 H<sub>2</sub>O molecules. As in tripodand TP, the centre of mass of MP is situated on the water side (Table 1), despite the hydrophobicity of three phenyl moieties attached to each phosphoryl group.

#### The positively charged $[LM^+]$ complexes (without counterion):

**The  $[222 \cdot K^+]$  and  $[TP \cdot Li^+]$  complexes:** These two complexes occupy a similar position at the interface. After the simulation, they are situated on the chloroform side, interacting with the water phase through “water fingers” made up of few H<sub>2</sub>O molecules. The complexed cation interacts differently with the solvent in  $[222 \cdot K^+]$  and  $[TP \cdot Li^+]$ . In the  $[222 \cdot K^+]$  complex, the cation is not completely shielded from the solvent and coordinates one water molecule, as in bulk water (Figure 3e). In the  $[TP \cdot Li^+]$  complex, the cation is encapsulated in the pseudocavity of the ligand and is completely shielded from the solvent. One H<sub>2</sub>O molecule is hydrogen bonded to one of the phosphoryl oxygen atoms (Figure 3d).

**The  $[MP \cdot K^+]$  complex:** The starting conformation of the complex was helixlike, with all oxygens of the ligand coordinated to the K<sup>+</sup> cation. Interactions with water molecules at the interface led first to an opening of the pseudocavity where the cation was situated, and then to dissociation of the complex. After dissociation, the MP ionophore remained at the interface, whereas K<sup>+</sup> diffused to bulk water.

**The  $[L \cdot M^+][X^-]$  and  $[L \cdot M^{2+}](X^-)_2$  neutral complexes:** *The  $[222 \cdot K^+][X^-]$  complexes:* In order to study the counterion ef-

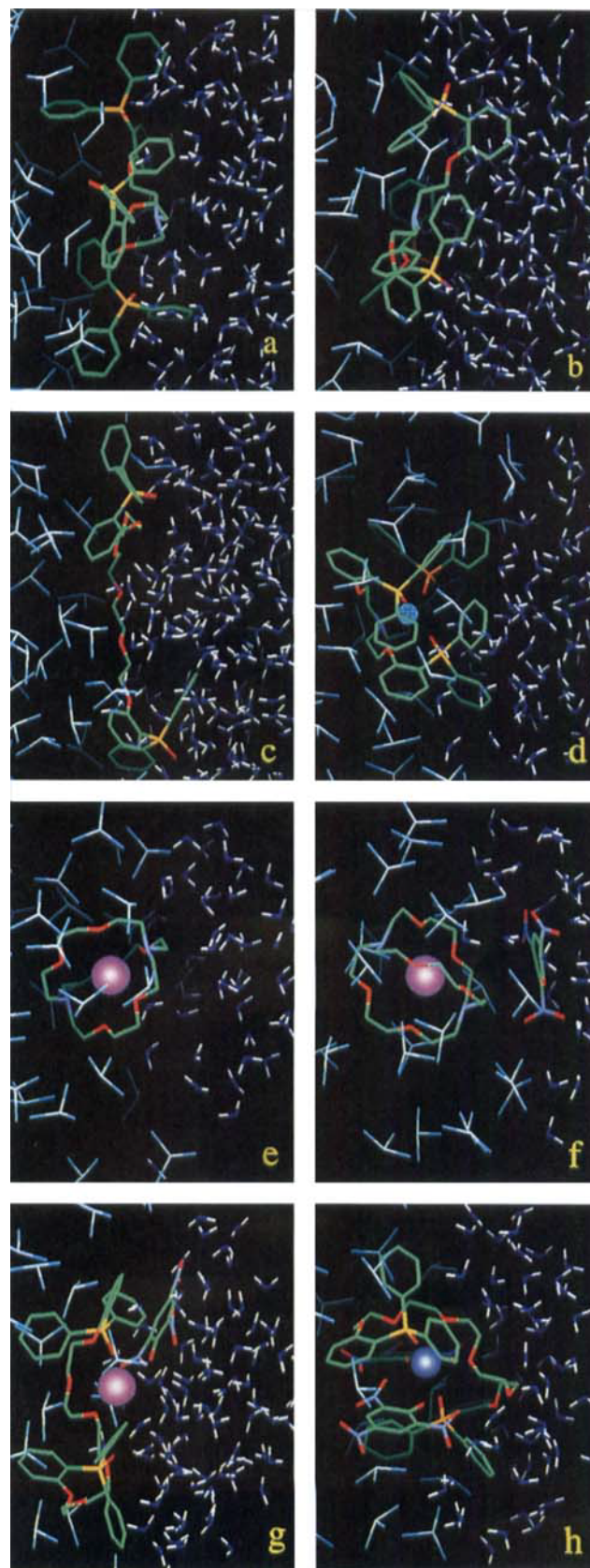


Figure 3. Snapshots of solutes at the water/chloroform interface, including selected solvent molecules. a) Starting structure of the tripodand TP (hydrophilic “open” conformation 1; see text). b) Final structure of TP uncomplexed. c) The free monopodand MP after 300 ps. d) The  $[TP \cdot Li^+]$  complex after 200 ps. e) The  $[222 \cdot K^+]$  complex after 450 ps. f) The  $[222 \cdot K^+][Pic^-]$  complex after 325 ps. g) The  $[MP \cdot K^+][Pic^-]$  complex after 300 ps. h) The  $[MP \cdot Sr^{2+}][Pic^-]_2$  complex after 500 ps.

fect on the adsorption pattern of the complexes at the interface, we simulated two  $[222 \cdot K^+ ]X^-$  complexes, where  $X^-$  is  $Cl^-$  (to model a "hard" lipophilic anion) or  $Pic^-$  (to model a "soft" hydrophobic anion). Initially both  $[222 \cdot K^+ ]$  and  $X^-$  were placed right at the interface. A different behaviour was observed with the two counterions. The  $Cl^-$  anion dissociated rapidly and migrated to the water phase. This contrasts with the  $Pic^-$  anion, which remained adsorbed at the interface, separated from  $K^+$  by two water molecules (Figure 3f).

**Migration of the  $[222 \cdot K^+ ]Pic^-$  complex from the bulk organic phase to the interface:** As the 222 cryptand is known to extract the  $K^+Pic^-$  salts from water to chloroform,<sup>[31]</sup> we paid particular attention to the stationary state observed computationally at the interface, to check whether this was not an artefact caused by the particular choice of the starting location of the solute. We therefore performed an additional simulation on the  $[222 \cdot K^+ ]Pic^-$  complex, starting in bulk chloroform. The centre of mass of the solute was initially placed at 20 Å from the interface, with the  $Pic^-$  anion further away from the interface than the  $[222 \cdot K^+ ]$  moiety. During the first 500 ps, the complex was found to diffuse and rotate in chloroform as an intimate ion pair, but not to approach the interface. The adsorption process started later and seemed to be driven by the anion. When the distance between  $Pic^-$  and the interface reached about 8 Å, the anion rapidly migrated to the interface, followed by the complexed cation (Figure 4). At the end of the simulation (850 ps), the position and solvation patterns of the complex are similar to those observed for the simulation starting with this solute at the interface (Table 1).

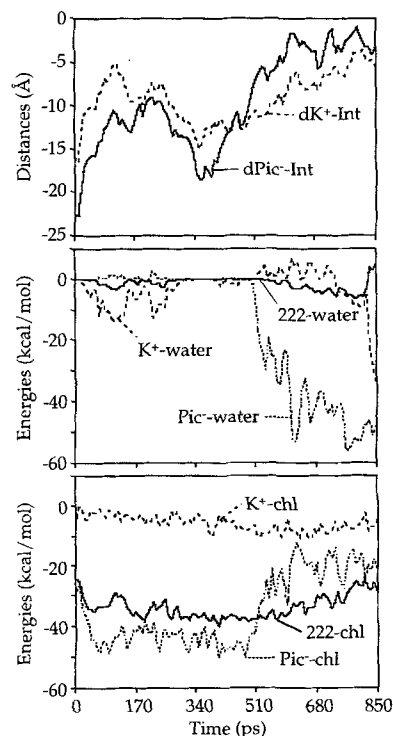


Figure 4. Analysis of the trajectory of the  $[222 \cdot K^+ ]Pic^-$  complex, starting in bulk chloroform: top: distance between the solute and the interface; middle: solute-water interaction energies; bottom: solute-chloroform interaction energies as a function of time.

The energy component analysis (Figure 4) shows that, at the interface,  $K^+$  and  $Pic^-$  ions experience attractive interactions with water, whereas the 222-water interaction energy is close to zero. The chloroform solvent interacts significantly with the ligand and the  $Pic^-$  anion (mostly through van der Waals forces), but interacts very weakly with  $K^+$ . Thus, to conclude this section, it is clear that the calculated adsorption at the interface is not an artefact caused by the choice of starting configuration, but is intrinsically preferred to solubilisation in the bulk organic phase.

**The  $[MP \cdot K^+ ]Pic^-$  complex:** In the starting structure,  $K^+$  was coordinated to the two phosphoryl oxygens ( $O_{ph}$ ), to four ether oxygens ( $O_{eth}$ ) of  $MP$ , and to two oxygens of the  $Pic^-$  anion. During the simulation, one  $O_{ph}$  and two  $O_{eth}$  atoms left the coordination sphere of  $K^+$  and the polyether chain unwrapped from around the cation. As a result of these conformational transformations, the  $K^+$  cation coordinates one water molecule. The  $Pic^-$  anion displays stacking interactions with the phenyl substituent of the terminal phosphoryl group bound to  $K^+$  (Figure 3g). The anion is situated at the interface between the water phase and the aromatic fragments of  $MP$ . We recall that, in the simulation on the  $[MP \cdot K^+ ]$  complex, dissociation was observed in the absence of counterion. The simulation on  $[MP \cdot K^+ ]Pic^-$  therefore demonstrates the importance of the picrate anion  $Pic^-$  (which is often used experimentally as a counterion in the extraction of cationic species) for the interfacial behaviour of the complex. It can be speculated that an anion like  $Cl^-$  would dissociate from the complex, diffuse to bulk water, while cation decomplexation would take place at the interface, as found for  $[MP \cdot K^+ ]$ .

**The  $[MP \cdot Sr^{2+} ](Pic^-)_2$  complex:** After 350 ps of simulations, most of this complex is situated in chloroform, but part of its polyether chain is on the water side of the interface. The  $Sr^{2+}$  cation remains complexed and completely shielded from both solvents. It coordinates two phosphoryl oxygens, two ether oxygens (instead of three in the gas phase<sup>[37]</sup>) and two oxygens of each  $Pic^-$  anion (Figure 3h).

## Discussion

At first glance, it might be surprising to find that species that are more soluble in an organic solvent than in water do not spontaneously migrate from the interface to chloroform. In this section we discuss *why*, *where* and *how* the interfacial adsorption of ionophores and their complexes takes place, with a particular focus on the question of counterion effect and on the hydrophobic/hydrophilic character of the complex.

**Adsorption of amphiphilic solutes at the water/organic interface—microscopic and macroscopic aspects:** Two complementary approaches—microscopic and macroscopic—can explain why the simulated ionophores and their complexes remain at the interface. From the microscopic point of view, the adsorption of the amphiphilic solute at the interface results from the interplay between solvent-solute and solvent-solvent interactions. The energy component analysis of the MD trajectories of related ionophores reported in references [24–28, 30] showed that the stationary states observed at the interface for macrocyclic ionophores are not driven by solute-solvent interaction energies. Indeed, the total attraction energy between the solute and the two liquid phases is smaller than, or comparable to, the interaction energy with bulk water and much smaller than the interaction energy with bulk chloroform. The second important energy component concerns the changes in solvent-solvent interactions and cohesive forces, which involve enthalpy and entropy components. It corresponds to the "cavitation energy", that is, to the work to be performed to form a cavity in the solvent upon immersion of the solute.<sup>[46]</sup> Although a quantita-

tive assessment is quite difficult, for a given solute, this energy cost is higher for water than for chloroform, in relation with their difference in surface tensions ( $72.9$  and  $26.7$  mN m<sup>-1</sup>, respectively).<sup>[12]</sup> The localisation of solutes in close vicinity to the interface, rather than in any of the bulk phases, may therefore be explained in terms of two main effects: 1) the lower energy cost for cavity formation in chloroform than in water and 2) the more efficient hydration of the amphiphilic solute at the interface than in the dry organic phase.

The phenomenological macroscopic approach relates the (algebraic) excess of interfacial concentration of the solute ( $c_{\text{surface}}$ ) relative to that in the bulk ( $c_{\text{bulk}}$ ) to the surface tension ( $\sigma$ ) by means of the Gibbs's adsorption theorem.<sup>[5, 12]</sup> When uncomplexed salts are added to a water phase,  $\sigma$  increases and  $c_{\text{surface}}$  is smaller than  $c_{\text{bulk}}$ . Conversely, when  $\sigma$  decreases,  $c_{\text{surface}}$  is larger than  $c_{\text{bulk}}$ . This is the case for amphiphilic molecules, and with extractants like ethers, alkylphosphoric acids and esters,<sup>[7]</sup> and crown ethers.<sup>[6, 8]</sup> The extent of adsorption depends on the concentration in the organic phase. For instance, with DB18C6 (dibenzo[18]crown-6), surface tension measurements suggest that for  $c_{\text{bulk}} > 0.5 \times 10^{-3}$  mol L<sup>-1</sup>, the water/benzene interface is fully covered by the ionophore.<sup>[6]</sup> In dilute solutions, there is a higher probability that such amphiphilic solutes will be situated at the interface than in the organic phase. Interestingly, in the case of tributylphosphate (TBP), studied at the water/*n*-decane interface, it was estimated that the enthalpy of adsorption at the interface is comparable to or somewhat larger than the enthalpy of migration from water to the organic phase (about  $-10.9$  and  $-10.3$  kcal mol<sup>-1</sup>, respectively).<sup>[4b]</sup> For a typical amphiphilic molecule like *n*-octanol, these numbers are respectively  $-7.4$  and  $-6.2$  kcal mol<sup>-1</sup>.<sup>[4b]</sup> This trend is fully consistent with our computational results and with simulations on TBP layers adsorbed at the chloroform–water interface.<sup>[48]</sup>

Another aspect of the macroscopic approach concerns the nature of the organic solvent *S*. When the polarity of *S* increases, the water/*S* interfacial tension decreases,<sup>[49]</sup> as does the interfacial excess  $\delta c = c_{\text{surface}} - c_{\text{bulk}}$ . As a result, the interface broadens and displays less affinity towards ionophores. This is again consistent with the results of MD simulations performed by Lauterbach et al. with the 1,3-alternate calix[4]-crown-6 ionophore at the water/*S* interface.<sup>[27]</sup> They showed that, when the polarity of chloroform (*S*) is increased by a factor of 2.0, the ionophore initially placed at the interface rapidly desorbs to *S*, whereas it remains adsorbed at the interface for more than 350 ps when a “standard” model is used for chloroform.<sup>[26, 27]</sup>

Another extreme situation is encountered when the surface tension of the nonaqueous phase *S* becomes much larger than the surface tension of water. In this case, the ionophore is predicted to adsorb at the interface on the water side. Related experimental results have been recently reported for the cryptand **222** and the  $[\mathbf{222} \cdot \text{Na}^+] \text{Cl}^-$  cryptate at the charged mercury–water interface.<sup>[45]</sup> As mercury has a larger surface tension than water ( $486$  and  $72.9$  mN m<sup>-1</sup>, respectively)<sup>[12]</sup>, the tension properties of the mercury–water interface are reversed, compared to chloroform–water. One remarkable result, however, is that the  $[\mathbf{222} \cdot \text{Na}^+] \text{cryptate}$  strongly adsorbs at the interface, despite the repulsive cryptate–cryptate interactions.<sup>[13]</sup>

**Electrostatic interactions as a driving force for diffusion from the organic phase to the interface:** The simulations on the  $[\mathbf{222} \cdot \text{K}^+] \text{Pic}^-$  complex migrating from the bulk chloroform to the interface provide interesting insights into the driving forces responsible for the diffusion from the bulk organic phase to the water/organic interface. The energy component analysis of the MD trajectory (Figure 4) shows that diffusion to the interface is mainly driven by electrostatic interactions between  $\text{Pic}^-$  and interfacial water molecules. When the solute is far enough away (about 20 Å), the average orientation of the water dipoles is more or less parallel to the interface as for the “neat” interface. As the cut-off distance used to calculate the nonbonded interactions is 12 Å, these water molecules do not interact with the solute in the simulation. However, as the anion approaches the interface (at less than 12 Å), water dipoles orient toward the organic phase and “switch on” the attraction between the interface and the solute. As a result, the  $\text{Pic}^-$  anion and some interfacial water molecules move toward each other (Figure 5) to form “water fingers” before formation of hydrogen bonds  $\text{H}_2\text{O} \cdots \text{Pic}^-$ . These observations are consistent with the results of Benjamin et al., who found a “leaking” of water from the interface toward the  $\text{Cl}^-$  anion, constrained at 6.5, 8.5 and 10.5 Å from the water/dichloroethane interface.<sup>[23]</sup> They also pointed out the importance of counterions in the interfacial adsorption of complexed ionophores.

Once the complex is at the interface, its interactions with water, which are mostly electrostatic in nature, prevent its migration back to the organic phase. Thus, from the computational point of view, it is stressed that the treatment of electrostatic interactions is very important. In particular, the effect of neglecting electrostatic interactions beyond the cut-off distance of 12 Å should be examined, as long-range electrostatic interactions modulate the energy components. They have been shown for instance to quantitatively determine the free energies of transfer of neutral solutes from chloroform to water.<sup>[50]</sup> At the interface, they are expected to stabilise the system when the polar solute is situated further away from the interface than the cut-off distance. In order to gain insight into this question, we performed a new MD simulation of the  $[\mathbf{222} \cdot \text{K}^+] \text{Pic}^-$  complex at the interface, using the Ewald option of AMBER 4.1. After 500 ps, the behaviour at the interface was nearly identical to the one obtained without Ewald. More quantitative insights will be obtained by comparison of the free energy profiles for interface crossing, with and without Ewald summation, which is presently under investigation in our laboratory. Based on the experimental results on the related extractant systems discussed above and on the analysis of our computational experiments, it can be concluded that long-range electrostatics does not critically



Figure 5. Diffusion of the  $[\mathbf{222} \cdot \text{K}^+] \text{Pic}^-$  complex from bulk chloroform toward the interface. Cumulated view at 506–516 ps showing selected interfacial water molecules. The chloroform molecules are omitted for clarity.

influence the strong tendency of the solutes to be adsorbed at the interface, at the concentrations simulated here.

**Dimensions of the interface:** Theoretical studies on “neat” water/organic liquid interfaces<sup>[15, 23–30]</sup> show that they are sharp at the molecular level and broadened by capillary waves. This is supported by experiment.<sup>[15]</sup> The thickness of the interface ( $\delta$ ) for the “neat” system was estimated as 6–9 Å.<sup>[28]</sup> Adsorption of ionophores and their complexes leads to an additional broadening of 2–6 Å due to the formation of “water fingers”. As a result, for ionophores or their complexes at small concentrations,  $\delta$  may reach 8–15 Å. At high concentrations, when the interface is saturated, ionophores and their complexes diffuse into the organic phase with some water molecules tightly bound to the solute (“water dragging effect”<sup>[15, 2]</sup>). This may dramatically increase the thickness of the interfacial region and may even lead to the formation of a macroscopic “third phase”.<sup>[2]</sup>

**Neutral vs. charged solutes at the interface—the “hydrophilic/hydrophobic” balance:** Based on the Kirkwood–Onsager theory, it might be anticipated that, as the total charge of the solute is increased, the attractive interactions with polar solvents are enhanced.<sup>[53]</sup> Therefore, at the interface, the solute is expected to move from the chloroform side to the water side, or even to completely migrate to bulk water. For molecular solutes like complexed ionophores  $[L \cdot M^{n+}]$ , the hydrophilic/hydrophobic character is, however, not so easy to predict. In principle, complexation of an  $M^{n+}$  cation makes the ligand L more hydrophilic, owing to the increase in charge. However, complexation generally involves conformational changes in L such that hydrophilic groups, diverging and well solvated in the free state, converge to  $M^{n+}$  in the complexed state, while hydrophobic groups become diverging. The ligand itself is therefore less well hydrated after complexation. In the following, we consider the changes in ligand interactions with water upon complexation, as an index related to the changes in hydrophilicity. For this purpose, the average water/complex ( $E_{ML+...w}$ ) and water/free ionophore ( $E_{L...w}$ ) interaction energies were calculated from MD trajectories in bulk water. We consider the absolute values  $|E_{ML+...w}|$  and  $|E_{L...w}|$  of  $E_{ML+...w}$  and  $E_{L...w}$ , respectively, and relate these to the differences in interfacial behaviour.

When free ligands are hydrophobic and display weak attractions with bulk water, they are expected to remain entirely in the organic phase, instead of being adsorbed at the interface. Upon complexation, however, attractions with water may increase ( $|E_{ML+...w}|$  becomes larger than  $|E_{L...w}|$ ), as may the adsorption properties. This can be illustrated by related experimental results on 1,10-phenanthroline and its derivatives. In their neutral state, these molecules do not display any significant adsorption at the water/chloroform interface, but are dissolved in the organic phase only.<sup>[54]</sup> In contrast, their protonated forms and their  $Fe^{II}$ ,  $Zn^{II}$  and  $Cu^{II}$  complexes exhibit remarkable interfacial activity.<sup>[54]</sup> Another illustration comes from computer experiments we recently performed on [(phenyldiamide)<sub>3</sub>·Eu<sup>3+</sup>] complexes at the water/chloroform interface. The complexes were found to migrate from the interface to bulk water, because of their high hydrophilicity.<sup>[55]</sup> On the other hand, the neutralised  $UO_2(NO_3)_2$  complexes of CMPO's remain at the interface,<sup>[30]</sup>

which again emphasises the important role of counterions on interfacial behaviour of complexed cations.

When the free ligand interacts better than its complex with water ( $|E_{L...w}| > |E_{ML+...w}|$ ), the solute becomes more lipophilic upon the complexation. This is the case for the free tripodand **TP** and its  $Li^+$  complex ( $E_{L...w}$  and  $E_{ML+...w}$  are  $-245$  and  $-141$  kcal mol<sup>-1</sup>, respectively). The uncomplexed **TP** is partitioned between the two liquid phases because of the efficient hydration of its phosphoryl groups, whereas the  $[TP \cdot Li^+]$  complex, which has no donor centres available for water molecules, stays entirely on the chloroform side of the interface, despite the +1 charge of the solute.

If the interaction energies  $E_{L...w}$  and  $E_{ML+...w}$  are similar, the charged complex and the neutral ionophores have similar interfacial behaviour. This is the case for the **222** cryptand (*K* form) and its  $[222 \cdot K^+]$  cryptate, which have similar interactions with bulk water ( $-79$  and  $-87$  kcal mol<sup>-1</sup>, respectively<sup>[32]</sup>) and display similar adsorption pattern. They both stay on the chloroform side of the interface. At a more quantitative level, it is noticeable that  $[222 \cdot K^+]$ , which interacts somewhat more with water than **222**, is situated closer to the interface (1.9 and 3.4 Å, respectively; Table 1).

This analysis thus makes clear that the precise location of the solutes at the interfaces is related to their “hydrophilic/hydrophobic” character. This cannot, however, be estimated in a straightforward manner, as it depends on the interplay between the charge and the conformation-dependent size, volume and solvent-accessible surface of the solute, which are solvent and environment dependent.<sup>[33]</sup> Counterions also contribute to the net charge of the adsorbed solute and to its lipophilic character (see next section).

#### Cation–anion interactions at the interface—where is the anion?

As stressed above, the cation and its counterion can both markedly determine the interfacial behaviour of extractant molecules, but no clear picture emerges from experiments. In fact, opposite views can be found in the literature. For instance, based on extraction studies on the  $[K^+ \cdot Pic^-]$  salt by DB18C6 to chloroform<sup>[6]</sup> or by [18]crown-6 and DB18C6 to benzene,<sup>[56]</sup> Danesi et al.<sup>[6]</sup> and Iosho et al.<sup>[56]</sup> suggested that the interfacial reaction of the  $Pic^-$  anion with the complexed  $K^+$  cation is slow and that cation–anion interactions are rather weak. This point of view was questioned later by Tarasov,<sup>[2]</sup> who considered the ion association in these systems to be a very fast reaction.

Our calculations at the interface show that the status of the anion results from the interplay between the cation–anion–solvent interactions. When the cation–anion interactions are strong (as in  $[MP \cdot Sr^{2+}](Pic^-)_2$ ), the ion pair remains intimate. When they are not, it dissociates. Depending on the lipophilicity of the anion, this dissociation leads either to solvent-separated ion pairs (as in the  $[222 \cdot K^+](Pic^-)$  complex) or to migration of the anion to water phase (as in the  $[222 \cdot K^+](Cl^-)$  complex). The larger affinity of an anion is for water, the less efficient are its interactions with the cation at the interface. This computational result is fully consistent with recent studies of Watarai et al. on the interfacial adsorptivity of  $[Fe(phenanthroline)_3]X_2$  complexes,<sup>[3]</sup> which show a clear reverse correlation between the reaction rate for ion pair formation and the hydration energies of anions  $X^-$  ( $ClO_4^- < CCl_3COO^- < Br^- < Cl^- < SO_4^{2-}$ ).

## Conclusions

We have reported MD simulations on three ionophores of different molecular topologies—the “chainlike” monopodand **MP**, the “octopuslike” tripodand **TP** and the bicyclic cryptand **222**—at the water/chloroform interface, represented explicitly, for timescales ranging from 200 to 850 ps. Simulations were performed on the free ionophores and on typical complexes with alkali and alkaline-earth metal cations, with or without  $\text{Pic}^-$  and  $\text{Cl}^-$  counterions.

All solutes were found to remain adsorbed at the interface, instead of migrating to bulk phases. They therefore behave as surfactants. This is consistent with available experimental data on related systems. This is also demonstrated on the computational side by recent PMF calculations on the free-energy profiles, which display a minimum at the interface.<sup>[57]</sup> A more detailed analysis reveals two basic types of situation at the interface, depending on the “hydrophilic/hydrophobic” balance. The solutes with more hydrophilic exterior (like free **MP** and **TP**, and the  $[\text{MP}\cdot\text{K}^+]\text{Pic}^-$  and  $[\text{MP}\cdot\text{Sr}^{2+}](\text{Pic}^-)_2$  complexes) are partitioned between the two liquid phases. Those that display a more hydrophobic exterior, like cryptand **222** and its complexes or the  $[\text{TP}\cdot\text{Li}^+]$  complex, stay almost entirely on the chloroform side of the interface and are partially hydrated by “water fingers”. The “hydrophilic/hydrophobic” character is, however, difficult to predict, as it depends not only on the total charge on the solute, but also on its conformation, which is itself modulated by the solvent and the environment.

We have found different situations for the ion pairs at the interface, depending on the interplay between  $\text{M}^{n+}\cdots\text{X}^-$  and  $\text{X}^-\cdots$ solvent interactions. Of particular interest is the fact that the lipophilic anion  $\text{Pic}^-$ , commonly used for extraction experiment, remains adsorbed at the interface with different relationships to  $\text{M}^{n+}$ , depending on the charge of the cation. This contrasts with the more hydrophilic  $\text{Cl}^-$  anion, which desorbs from the interface and diffuses to bulk water. It is thus speculated that amphiphilic anions, like those of fatty acid derivatives, play an important role in determining the nature of the complexes adsorbed at the interface, and on the precise sequence of events that occur during extraction or transport. We suggest this to be an important feature of the related synergistic effects.

This study calls for further investigations. On the theoretical side, the force-field limitations and protocols for calculations have to be refined. Some recently reported studies<sup>[27]</sup> do, however, rule out a number of possible artefacts that could bias the qualitative conclusions drawn here. On the experimental side, there are, to the best of our knowledge, surprisingly few studies on the interfacial behaviour of macrocyclic ionophores. In addition to interfaces between pure liquids, interfaces with molecular ordering, like micelles and microemulsions,<sup>[58]</sup> should be studied. Electrochemical studies should also tell us more about ion-crossing through interfaces.<sup>[11]</sup>

Once adsorption at the liquid–liquid interface has been acknowledged to be an important feature, an important question remains to be discussed in the context of ion extraction and transport processes, namely, why and when does the complexed ion diffuse into the organic phase? Diffusion takes place when the concentration of the complexes and of the ionophores is high enough. This will be addressed in a future publication, based on

computer experiments, where the interface is saturated with free ionophores (e.g. [18]crown-6) or with complexes (e.g.  $[\text{K}^+\cdot[18]\text{crown-6}]\text{Pic}^-$  and  $[\text{K}^+\cdot\text{MP}](\text{Pic}^-)_2$ ).<sup>[58]</sup> After saturation of the interface, slow desorption and diffusion to the organic phase are found to take place. Such simulations are relatively demanding on computer time. However, with the increased computer power and software developments, it is hoped that theoretical approaches such as the one used here will contribute to our understanding of the factors that influence the interactions of solutes in complex environments such as liquid–liquid interfaces and the selective extraction (“recognition”) of metal ions. These studies also have bearing on surface properties of complexant molecules in contact with organised systems, like micelles, microemulsions and lamellar phases,<sup>[59]</sup> and on related fields such as phase-transfer catalysis,<sup>[10]</sup> electrochemistry<sup>[11]</sup> and ion-crossing through membranes.<sup>[60]</sup>

**Acknowledgements:** CNRS and IDRIS are acknowledged for allocating computer time. AV and GW thank INTAS for the research grant 94-3249 and E. Engler for software developments. GW thanks the EU COST-D7 action for support.

Received: August 16, 1996 [F 445]

- [1] P. R. Danesi in *Principles and Practices of Solvent Extraction* (Eds: J. Rydberg, C. Musikas, G. R. Choppin), Marcel Dekker, New York, 1992; pp. 157–208.
- [2] V. V. Tarasov, G. A. Yagodin, A. A. Pichugin, *Kinetics of the Extraction of Inorganic Compounds (Russ)*, VINITI, Moscow, 1984, pp. 171. G. A. Yagodin, V. V. Tarasov, *Solvent Extr. Ion Exch.* 1984, 2, 139–179.
- [3] H. Watarai, *Trends Anal. Chem.* 1993, 12, 313–318.
- [4] a) V. V. Tarasov, A. V. Fomin, G. A. Yagodin, *Zh. Fizich. Khimii (Russ)* 1971, 45, 1300. b) N. H. Sagert, W. Lee, M. J. Quinn, *Can. J. Chem.* 1979, 57, 1218–1223. c) G. F. Vandegrift, E. P. Horwitz, *J. Inorg. Nucl. Chem.* 1977, 39, 1425–1432.
- [5] N. K. Adam, *Physics and Chemistry of Surfaces*, 3rd ed., Oxford University Press, Oxford, 1941.
- [6] P. R. Danesi, R. Chiarizia, M. Pizzichini, A. Satelli, *J. Inorg. Nucl. Chem.* 1978, 40, 1119–1123.
- [7] V. V. Tarasov, G. A. Yagodin, *Extraction Kinetics (Russ)*, VINITI, Moscow, 1974, pp. 119.
- [8] P. R. Danesi, R. Chiarizia, *CRS Critical Reviews in Analytical Chemistry* 1980, 10, 1–126. T. M. Fyles, *J. Chem. Soc. Faraday Trans. 1*, 1986, 82, 617–633.
- [9] G. A. Yagodin, S. Z. Kagan, V. V. Tarasov, A. V. Ochkin, O. A. Sinegribova, V. V. Sergievsky, V. G. Vygon, *Solvent Extraction (Russ)*, Khimiya, Moscow, 1981, pp. 399.
- [10] W. Lasek, W. Makosza, *J. Phys. Org. Chem.* 1993, 6, 412–420. C. M. Starks, C. L. Liotta, M. Halpern in *Phase Transfer Catalysis* (Ed.: C. M. Starks), Chapman & Hall, New York, 1994.
- [11] P. Vanyssek, *Electrochimica Acta* 1995, 40, 2841–2847. W. Schmickler, *Interfacial Electrochemistry*, Oxford University Press, Oxford, 1996. H. H. J. Girault, D. J. Schriffin, *Electroanalytical Chemistry* (Ed.: A. J. Bard Dekker), New York, 1989. *Spectroscopic and Diffraction Techniques in Interfacial Electrochemistry* (Eds.: C. Gutierrez, C. Melendres), NATO ASI Series Vol. 320, Kluwer, Dordrecht, 1990. *The Interface Structure and Electrochemical Processes at the Boundary between Two Immiscible Liquids* (Ed.: V. E. Kazarinov), Berlin, 1987.
- [12] A. Adamson, *Physical Chemistry of Surfaces*, Wiley Interscience, New York, 1990; see also P. C. Hiemenz, *Principles of Colloid and Surface Chemistry*, 2nd ed., M. Dekker, New York, 1986.
- [13] R. R. Naujok, H. J. Paul, R. M. Corn, *J. Phys. Chem.* 1996, 100, 10497–10507.
- [14] T. Takenaka, T. Nakagana, *J. Phys. Chem.* 1976, 80, 475–480. R. P. Sperline, H. Freiser, *Langmuir* 1990, 6, 334.
- [15] P. Linse, *J. Chem. Phys.* 1987, 86, 4177–4187.
- [16] J. Gao, W. L. Jorgensen, *J. Phys. Chem.* 1988, 92, 5813–5822.
- [17] I. L. Carpenter, W. J. Hehre, *J. Phys. Chem.* 1990, 94, 531–536.
- [18] D. Michael, I. Benjamin, *J. Phys. Chem.* 1995, 99, 1530–1536.
- [19] A. R. van Buuren, S.-J. Marrink, H. J. C. Berendsen, *J. Phys. Chem.* 1993, 97, 9206–9212.
- [20] M. A. Wilson, A. Pohorille, *J. Am. Chem. Soc.* 1994, 116, 1490–1501. See also B. Smit, *Phys. Rev. A*, 1988, 37, 3431. K. Esselink, P. A. J. Hilbers, S. Karaborni, J. L. Siepmann, B. Smit, *Molecular Simulation*, 1995, 14, 259–274 and references therein.
- [21] C. Y. Lee, J. A. McCammon, P. J. Rossky, *J. Chem. Phys.* 1984, 80, 4448–4455.



- [22] W. Guba, H. Kessler, *J. Phys. Chem.* **1994**, *98*, 23–27. See also W. Guba, R. Haessner, G. Breipohl, S. Henke, J. Knolle, V. Santagada, H. Kessler, *J. Am. Chem. Soc.* **1994**, *116*, 7532–7540.
- [23] K. J. Schweighofer, I. Benjamin, *J. Phys. Chem.* **1995**, *99*, 9974–9985. I. Benjamin, *Science*, **1993**, *261*, 1558–1560.
- [24] A. Varnek, G. Wipff, *J. Comput. Chem.* **1996**, *17*, 1520–1531.
- [25] A. Varnek, C. Sirlin, G. Wipff, in *Crystallography of Supramolecular Compounds* (Ed.: G. Tsoucaris), NATO ASI Series Vol. C480, Dordrecht, **1996**, pp. 67–99.
- [26] M. Lauterbach, G. Wipff, *Supramol. Chem.* **1995**, *6*, 187–207.
- [27] M. Lauterbach, G. Wipff, *Liquid–Liquid Extraction of Alkali Cations by Calix[4]Crown Ionophores: Conformation-Dependent Na<sup>+</sup>/Cs<sup>+</sup> Binding Selectivity. A MD FEP Study in Pure Chloroform and MD Simulations at the Water/Chloroform Interface in Physical Supramolecular Chemistry* (Ed.: L. Echegoyen), NATO ASI Series, Kluwer, Dordrecht, **1996**, pp. 65–102.
- [28] G. Wipff, E. Engler, P. Guilbaud, M. Lauterbach, L. Troxler, A. Varnek, *New. J. Chem.* **1996**, *20*, 403–417.
- [29] I. Benjamin, *J. Chem. Phys.* **1992**, *97*, 1432–1445 and **1992**, *96*, 577–585.
- [30] P. Guilbaud, G. Wipff, *New J. Chem.* **1996**, *20*, 631–642.
- [31] B. Dietrich, P. Viout, J.-M. Lehn, *Macrocyclic Chemistry*, VCH, Weinheim, **1993**, pp. 371. J.-P. Behr, M. Kirch, J.-M. Lehn, *J. Am. Chem. Soc.* **1985**, *107*, 241–246.
- [32] P. Auffinger, G. Wipff, *J. Am. Chem. Soc.* **1991**, *113*, 5976–5988. P. Auffinger and G. Wipff, *J. Chimie Phys.* **1991**, *88*, 2525–2534.
- [33] L. Troxler, G. Wipff, *J. Am. Chem. Soc.* **1994**, *116*, 1468–1480. G. Wipff, L. Troxler in *Computational Approaches in Supramolecular Chemistry* (Ed.: G. Wipff), NATO ASI Series Vol. C426, Kluwer, Dordrecht, **1994**, pp. 319–348.
- [34] J. Åqvist, *J. Phys. Chem.* **1990**, *94*, 8021–8024.
- [35] V. Bauhin, V. Soloviev, A. Varnek, G. Wipff, unpublished results. Concerning the nomenclature, **MP** can be considered either as a monopodand or as a dipodand. The latter description applies when the central ether oxygen acts as an anchoring group, which may not be the case here (E. Weber and F. Vögtle, *Crown-Type Compounds—An Introductory Overview in Host–Guest Complex Chemistry I, Topics Current Chemistry*, Springer, Berlin, **1981**, p. 3).
- [36] L. Cecille, M. Casarci, L. Pietrelli, *New Separation Chemistry Techniques for Radioactive Waste and other Specific Applications*, Elsevier, London, **1991**.
- [37] A. Y. Nazarenko, A. Varnek, G. Wipff, unpublished results.
- [38] A. Varnek, G. Morosi, A. Gamba, *J. Phys. Org. Chem.* **1992**, *5*, 109–118.
- [39] D. A. Pearlman, D. A. Case, J. C. Cadwell, G. L. Seibel, U. C. Singh, P. Weiner, P. A. Kollman, *AMBER4*, University of California, San Francisco, **1991**.
- [40] S. J. Weiner, P. A. Kollman, D. A. Case, U. C. Singh, C. Ghio, G. Alagona, S. Profeta, Jr., P. Weiner, *J. Am. Chem. Soc.* **1984**, *106*, 765. S. J. Weiner, P. A. Kollman, D. T. Nguen, D. A. Case, *J. Comput. Chem.* **1986**, *7*, 230.
- [41] *SPARTAN, Version 4.0.4, Wavefunction* **1995**.
- [42] W. L. Jorgensen, J. Chandrasekhar, J. D. Madura, *J. Chem. Phys.* **1983**, *79*, 926–935.
- [43] W. L. Jorgensen, J. M. Briggs, M. L. Contreras, *J. Phys. Chem.* **1990**, *94*, 1683–1686.
- [44] E. Engler, G. Wipff, *MD-DRAW. A Program for Graphical Representation of a Molecular Trajectories*, Université Louis Pasteur, Strasbourg, **1992**. See *Crystallography of Supramolecular Compounds* (Ed.: G. Tsoucaris), NATO ASI Series Vol. C480, Kluwer, Dordrecht, **1996**, pp. 461–476. E. Engler, G. Wipff, *MDS. A Program to Analyze MD Trajectories*, unpublished.
- [45] M. Carlà, C. M. C. Gambi, P. Baglioni, *J. Phys. Chem.* **1996**, *100*, 11067–11071.
- [46] B. Guillot, Y. Guissani, S. Bratos, *J. Chem. Phys.* **1991**, *95*, 3643. A. Wallqvist, *J. Phys. Chem.* **1991**, *95*, 8921–8927. W. Blokzijl, J. B. F. N. Engberts, *Angew. Chem. Int. Ed. Engl.* **1993**, *32*, 1545. A. Pohorille, L. R. Pratt, *J. Am. Chem. Soc.* **1990**, *112*, 5066–5074. R. A. Pierotti, *Chem. Rev.* **1976**, *76*, 717–726. M. Prevost, I. T. Oliveira, J.-P. Kocher, S. J. Wodak, *J. Phys. Chem.* **1996**, *100*, 2738–2743 and references therein.
- [47] R. Avayard, B. Vincent, *Prog. Surf. Sci.* **1977**, *8*, 59. R. Avayard, R. W. Mitchell, *Trans. Farad. Soc.* **1969**, *65*, 2645–2653.
- [48] P. Beudaert, G. Wipff, unpublished results.
- [49] R. C. Weast, *CRC Handbook of Chemistry and Physics*, CRC Press, Cranwood Parkway, Cleveland, **1978**.
- [50] X. Daura, P. H. Hünenberger, A. E. Mark, E. Querol, F. X. Avilés, W. F. van Gunsteren, *J. Am. Chem. Soc.* **1996**, *118*, 6285–6294.
- [51] C. Wei, A. J. Bard, M. V. Mirkin, *J. Phys. Chem.* **1995**, *99*, 16033–16042.
- [52] R.-S. Tsai, W. Fan, N. E. Tayar, P.-A. Carrupt, B. Testa, L. B. Kier, *J. Am. Chem. Soc.* **1993**, *115*, 9632–9639. W. Fan, R.-S. Tsai, N. E. Tayar, P.-A. Carrupt, B. Testa, *J. Phys. Chem.* **1994**, *98*, 329–333.
- [53] J. Tomasi, M. Persico, *Chem. Rev.* **1994**, *94*, 2027–2094 and references therein.
- [54] H. Watarai, Y. Shibuya, *Bull. Chem. Soc. Jpn.* **1989**, *62*, 3446–3450.
- [55] L. Giovannino, G. Wipff, unpublished results.
- [56] M. Ioshio, H. Noguchi, K. Inoue, in *Proc. Int. Solv. Extr. Conf. (ISEC-83)*, Denver, Colorado, USA, 1983, pp. 309–310.
- [57] M. Lauterbach, G. Wipff, unpublished results. M. Lauterbach, *Simulation par ordinateur de l'extraction liquide-liquide des cations alcalins par des ionophores de type calixarène-couronne et valinomycine*, PhD Thesis, Université Louis Pasteur de Strasbourg, **1996**.
- [58] L. Troxler and G. Wipff, *MD Simulations of Ionophores Free and Complexed at a Water–Chloroform Interface*, poster presented at the XXI International Symposium on Macrocyclic Chemistry, **1996**, Montecatini, Italy.
- [59] K. Monserrat, M. Graetzl, P. Tundo, *J. Am. Chem. Soc.* **1980**, *102*, 5527–5529. Y. C. Liu, P. Baglioni, J. Teixeira, S. H. Chen, *J. Phys. Chem.* **1994**, *98*, 10208–10215, and references therein.
- [60] B. H. Honig, W. L. Hubbel, R. F. Flewelling, *Annu. Rev. Biophys. Biophys. Chem.* **1986**, *15*, 163. R. B. Gennis, *Biomembranes*, Springer, New York, **1989**. Y. Shao, H. H. Girault, *J. Electroanal. Chem.* **1990**, *282*, 59.